Full Length Research Paper

Using electrical impedance tomography in following up skin conductivity change for different sonophoresis conditions

Mamdouh M. Shawki* and Abdel-Rahman M. Hereba

Bio-Medical Physics Department, Medical Research Institute, Alexandria University, Egypt.

Sonophoresis is the using of ultrasound waves to increase the entrancement of genes and drugs surpassing the skin barrier. Many mechanisms have been described to illustrate the sonophoresis mode of action; some describe changes in skin resistance during sonophoresis. Electrical impedance tomography (EIT) technique uses voltage measurement through a group of electrodes and reconstructs the data to a conductivity picture. The aim of this work is to evaluate the possibility of using EIT in order to detect changes in mice skin conductivity under pulsed ultrasound waves with powers of 1 and 3 W/cm^2 and times of exposure of 2, 4, and 6 min. EIT system was designed and performed locally. The mice skin was obtained from ten albino mice. Immediately after the skin part was exposed to certain sonophoretic condition, its complex biological impedance was measured using the EIT device. The resultant pictures then were analysed using special software. The results indicate that EIT can be used as a good technique for skin conductivity scan. The data analysis shows that as the ultrasound power increases, the skin conductivity increases. However, there is no significant decrease in skin impedance with time in the same ultrasound power at the time range used.

Key words: Electrical impedance tomography (EIT), sonophoresis, skin conductivity.

INTRODUCTION

Transdermal drug delivery offers several advantages, particularly for those drugs that when taken orally are lost due to gastrointestinal and liver metabolism (first-pass effect) (Hadgraft and Guy, 1989). However, because of the presence of the stratum corneum, the outermost layer of the skin is generally impermeable, especially to large and/or hydrophilic molecules such as peptides and proteins (Schaefer and Redelmeier, 1996). To increase the transdermal drug delivery rate to therapeutically signi-ficant levels, various chemical and physical approaches have been investigated, including chemical enhancers (Johnson et al., 1997), electric fields (iontophoresis (Takasuga et al., 2011) and electroporation (Prausnitz et al., 1993), and ultrasound waves (sonophoresis) (Polat et al., 2011). Sonophoresis is a process that exponentially increases the absorption of topical compounds (transdermal delivery) into the epidermis, dermis and skin appendages. Sonophoresis occurs because ultrasound waves stimulate micro-vibrations within the skin epidermis and increase the overall kinetic energy of molecules making up topical agents. It is widely used in hospitals to deliver drugs through the skin by mixing them with a coupling agent (gel, cream, ointment) that transfers ultrasonic energy from the ultrasound transducer to the skin (Pahade et al., 2010).

Cavitation, temperature elevation, acoustic streaming and convective dispersion are believed to be factors that may substantially contribute to the efficacy of ultrasound. Cavitation effects are generally recognized to be the dominant mechanism of sonophoretic enhancement. These effects are directly related to the observed drop in the electrical resistance of the skin. Due to significant hindrance of the ionic transport through the lipid bilayers,

---

*Corresponding author. E-mail: mamdouh971@hotmail.com. Tel: +2(03)4285455. Fax: +2(03)4283719
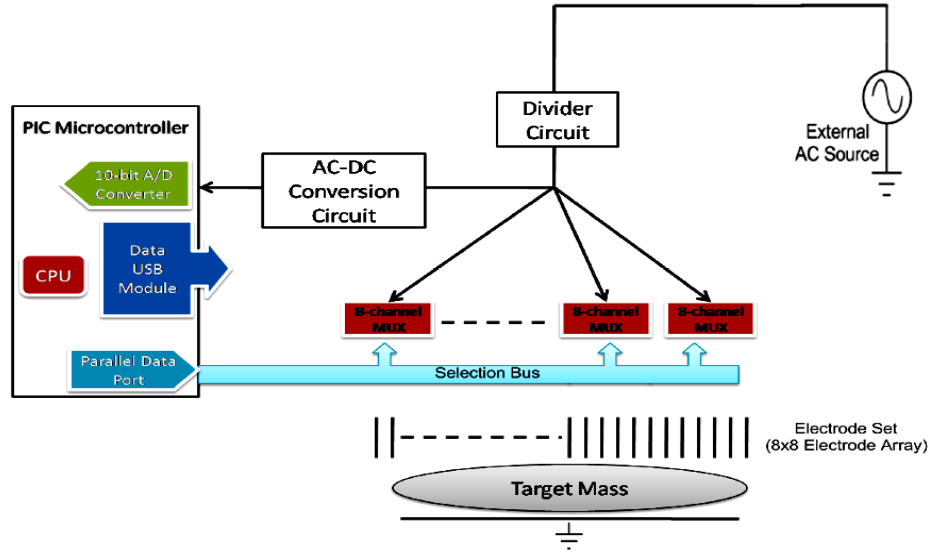
Figure 1. System block diagram.

the electrical resistance of the skin is very high and it has been used to verify that the structural integrity of skin samples is within the normal range. However, the continuous monitoring of skin electrical resistance during ultrasound application can provide insight into the mechanisms governing the enhancement of mass transfer through this biological barrier (Bagshaw et al., 2003). Electrical impedance tomography (EIT) is a noninvasive technique whereby images of the conductivity within a body can be reconstructed from voltage measurements made on the surface (Cheneyy et al., 1993). Electrodes are attached to the body in a fashion similar to electroencephalography (EEG), and each measurement is typically made from a combination of four electrodes, two to inject current and two to sample the resulting voltage distribution (Costaa et al., 2009).

For a particular pair of current injection electrodes, several voltage measurements are taken, the injection pair is then switched, and the process repeated to produce one complete data set. A reconstruction algorithm is used to relate the measured voltages to the conductivity within the body (Metherall et al., 1996). In EIT, the hardware usually will be set to measure with a sampling rate of 10 to 25 per second and for a period of 30 to 60 s. Thus, each measurement session consists of several hundreds of single tomograms. The pixel values in the tomograms approximate local resistivity. The pixel values equal relative impedance change (dimensionless unit), a value that is derived either from a baseline measurement or from parts of the actual measurement itself (Bodenstein et al., 2009).

Tang et al. (2001) illustrated the relationship between permeability of a hydrophilic permeant (P_{diff}) through a skin, and the skin conductivity (σ) by the following equations:

$$P_{diff} = C * \sigma / \Delta x \tag{1}$$

$$C = (kT/ 2z^2 f c_{ion} e_0) \times (D^\infty_p H \lambda_p) / (D^\infty_{ion} H \lambda_{ion}) \tag{2}$$

Here: Δx is skin thickness, C is constant, z is the electrolyte valence, F is the Faraday constant, c_{ion} is the electrolyte molar concentration, e_0 is the electronic charge, K is the Boltzmann constant, and T is the absolute temperature. D^∞_{ion} and D^∞_p are the diffusion coefficients at infinite dilution for ion and permeant respectively. $H(\lambda_{ion})$ and $H(\lambda_p)$ are the diffusion hindrance factors for ion and permeant respectively.

Substituting skin resistivity $(R) = \Delta x / \sigma$ (3)

$$Log P_{diff} = Log C - Log R \tag{4}$$

The aim of this study is to evaluate the role of EIT technique in the detection of the change in skin conductivity due to different sonophoresis powers and times of exposures, which in turn according to equation (4) gives direct relation with solute permeability.

MATERIALS AND METHODS

Constructing of electrical impedance tomography system

The device parts

The system was constructed locally at the Bio-Physics Department, Medical Research Institute, Alexandria University. The system block diagram is illustrated in Figure 1.

Data acquisition system: It is a microcontroller-based system responsible for data collection and interfacing; the system is based

Figure 2. Device main panel view.

on a Microchip PIC high performance microcontroller (part no: PIC18F4550). The data acquisition process is performed by applying an external AC voltage to a simple voltage divider circuit where the applied voltage is divided between a constant value resistor and the target mass impedance at a specific electrode.

Voltage measurement: The AC voltage across the electrode is converted to an equivalent DC voltage through a simple AC-DC conversion circuit (full wave rectifier + RC filter). The analog DC voltage is then converted to a digital value using the integrated analog to digital converter module. The A/D converter has 10-bit resolution of the digital result, 5 V of reference voltage and voltage sensitivity of 4.89 mV. These values guarantee an accurate measurement of the analog DC voltage. The value of the measured DC voltage is indicative of the magnitude of the bioelectrical impedance.

Electrode multiplexing: The electrode set (64 electrodes) is multiplexed using a set of 8-to-1 channel multiplexers, so that the voltage across each electrode is measured independently. The multiplexing system is then a set of 8 multiplexers; each set is targeting 8 electrodes. The microcontroller activates one of the multiplexers and then sends the selection data (for the channel selection within the same multiplexer) to gain the access to one electrode while disabling the other 63 ones. The analog voltage across the selected electrode is converted to the corresponding DC value using the AC/DC converter circuit. The DC voltage is measured and then converted to a digital value using the 10-bit A/D converter module.

Data delivery: The digital value for each voltage is transmitted via the built-in USB module. This digital value is then used to generate the tomographic image on the target computer.

Image reconstruction system

It is a software-based system responsible for data handling and tomographic image generation. The developed software is split into two main interconnected components; Data acquisition software (VB.NET based) and image generating software (MATLAB based).

Data acquisition software: This part of the software (namely: Bio-Image Scanner V2.0) was developed using (Microsoft Visual Basic .NET) to perform, control the hardware data acquisition system via the computer's USB HID (Human Interface Device), collect, and store data elements corresponding to each member of the electrode set. The software sends an asynchronous message to the data acquisition system via USB, forcing it to start its operation (multiplex, read, send, etc.). The data acquisition system responds

with a stream of data (64 units) representing the data from the electrode set, then the software waits for this data stream to store it and export it to the last stage (image generating software).

Data exporting mechanism: On the read of a new data unit, the software saves this unit in an ASCII-formatted text file using the .NET file system capabilities. When the data stream ends, the software starts the image generating executable (plot_impedance.exe) via a simple communication with the windows shell.

Image generation software: This part of the software (namely: plot_impedance.exe) was developed (using MATLAB 7.5) to perform reordering of imported data elements, performing linear data interpolation, and generating a tomographic image using a predefined color code. The software reads the text file that was created by the data acquisition software and translates the text contents into "double" format, creates a matrix of integers with the size of 8x8 (each matrix element corresponds to an electrode), then performs 2D linear data interpolation between the data elements resulting into a new matrix with the size of (700x700) data elements, and finally the (700x700) 2D matrix is plotted using filled contours to output an image.

Device features and general description

The device has an internal power supply unit and operates on 220V AC; it has 2 BNC connectors, one for the ground-connected metal slab and another for the AC input from a standard function generator. The device main panel view is shown in Figure 2.

Device interface: The Bio-image scanner uses a full speed USB 2.0 interface for communications and data transfer. The device is connected to the USB hub using a USB cable.

Operation setup: The output of the function generator was adjusted to 9V Sine wave and the frequency range (typically 100 KHz) was chosen. The output resolution was optimized for 9V AC input, so that any change may cause the output image to have a bad color resolution, both BNC connectors of the AC input and the GND metal Slab were connected, the device to the USB hub using a USB cable was connected, and then the device was powered on, so that the "Bio Image Scanner v2.0" program could be run.

Sonophoresis on mice skin

Ten albino mice aged 8 to 10 weeks and weighing between 20 to 25 g (obtained from animal house, Medical Research Institute,
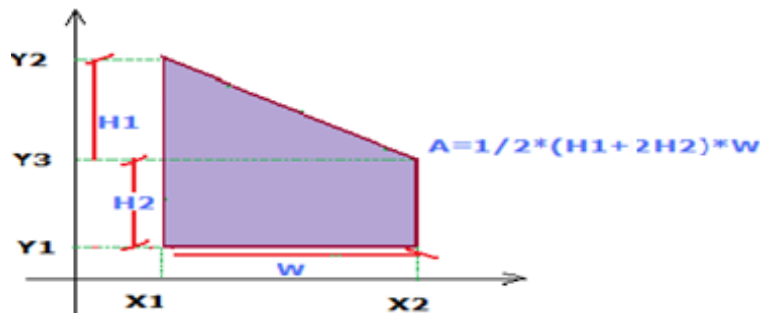
Figure 3. The idea of polygon area calculation.
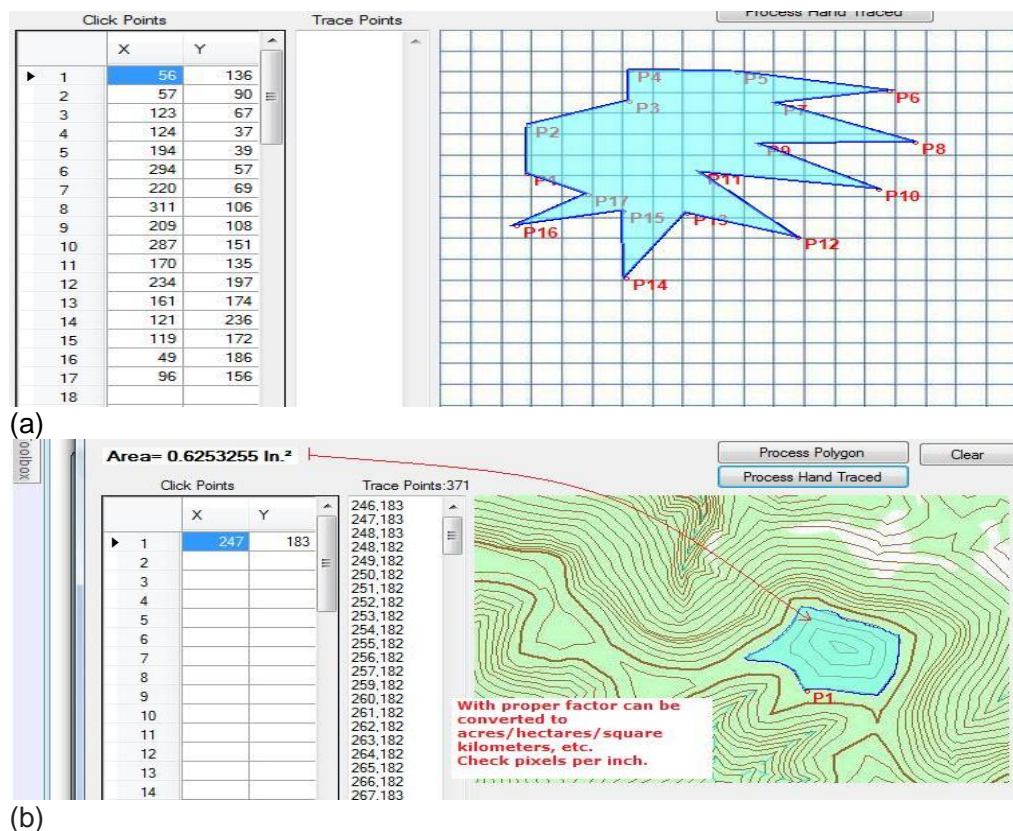

(a)

(b)

Figure 4. (a) and (b) Shows the steps of area of polygon program operation.

Alexandria University) were anesthetized and sacrificed and the whole skin was excised and sliced into equal pieces using a scalpel approximately 3 cm in length, 3 cm in width, and 8 mm in thickness. 35 skin samples were obtained of approximately equal volumes. Experiments were conducted within 90 min from animal sacrifice with the tissue stored in 0.9% NaCl at room temperature until use. The skin samples were randomly classified into seven groups; each of five samples. Control group was not exposed to ultrasound waves. Three groups were exposed to pulsed ultrasound waves (Ultrasonic Therapeutic Apparatus CSL-1, made in China) 800 KHz, 1 W/cm^2 for 2, 4, and 6 min, respectively. The remaining three groups were exposed to the same ultrasonic apparatus but at 3 W/cm^2 for 2, 4, and 6 min, respectively. Immediately after the exposure time, each sample was examined using the electrical impedance tomography device.

Designing special program for area calculation of images of irregular shapes

Private program was designed by a specialist to determine the area of the different irregular shapes in each picture which was called area of polygon program. The programming language is C-Sharp, and the development enrolment is visual studio.net 2008. The idea of obtaining the area is to move from point to point on a path and use trapezium areas. These areas are the shadow under the line that connects two consecutive points on a Cartesian chart. The idea is shown in Figure 3. An irregular area needs plenty more points in the path to be defined, but the process is the same. The creation of the path depends on the type of shape. On the program, the picture box was clicked on and the array list was filled. Then the data grid appeared when creating the path for a polygon, as shown in Figure 4.
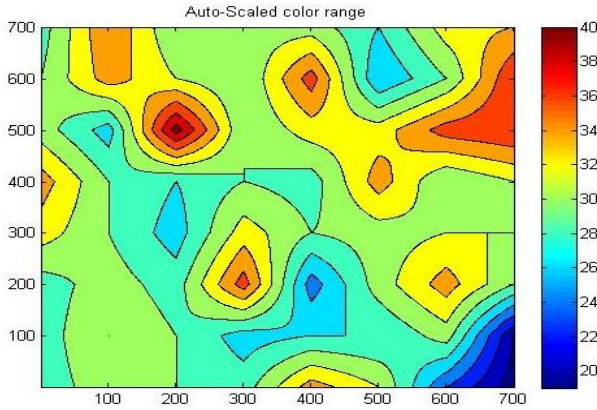
Figure 5. Electrical bio-impedance tomography picture for control skin: 2D linear data interpolation with the size of (700x700) data elements.
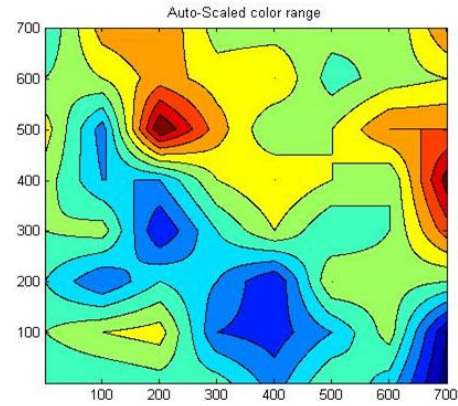

Figure 6. Electrical bio-impedance tomography picture for skin exposed to US, 1 W/cm^2, for 2 min: 2D linear data interpolation with the size of (700x700) data elements
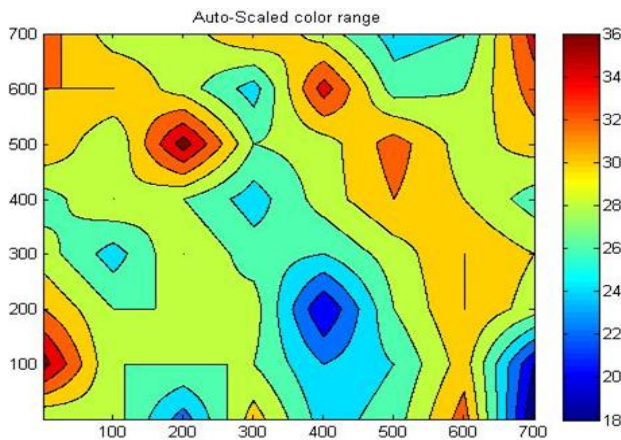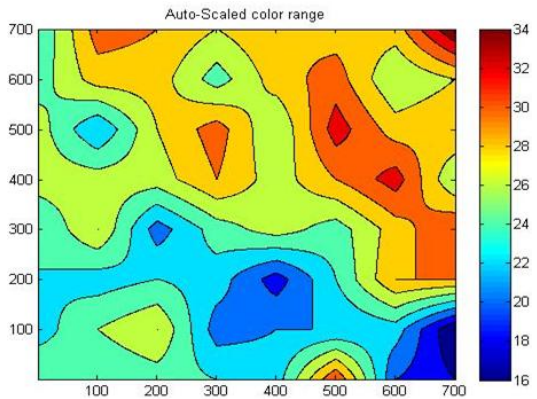
Complex bioelectrical impedance calculation

The complex impedance was calculated as a result of each image colors area processing (using area of polygon software) by calculating the area percentage of each color regarding to the total skin EIT picture area then multiply the value in the corresponding impedance. The total impedance of the sample is the sum of the whole picture parts impedances. Analysis for five samples (pictures) from each group was done. Impedance averages and standard deviations were calculated for each group. One-way analysis of variance (ANOVA) was used to compare each variable in the different studied groups. For all statistical comparisons, a value of $p < 0.05$ was considered significant.

RESULTS

Figures 5 to11 show examples of bioelectrical impedance tomography pictures for each examined group with color legend for the impedance. Color area calculation done by area of polygon software is placed on Figure 11 as an
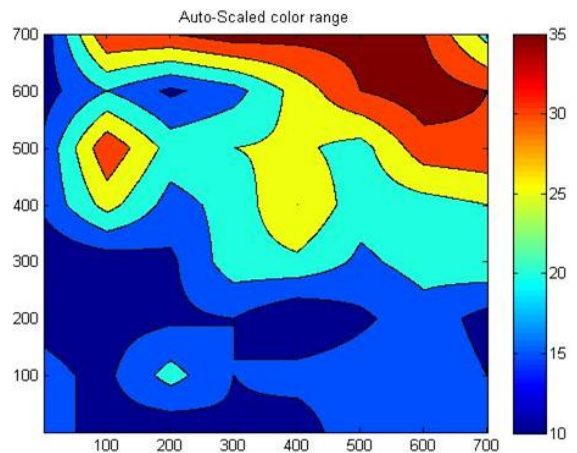

Figure 7. Electrical bio-impedance tomography picture for skin exposed to US, 1 W/cm^2, for 4 min: 2D linear data interpolation with the size of (700x700) data elements.

Figure 8. Electrical bio-impedance tomography picture for skin exposed to US, 1 W/cm^2, for 6 min: 2D linear data interpolation with the size of (700x700) data elements.

Figure 9. Electrical bio-impedance tomography picture for skin exposed to US, 3 W/cm^2, for 2 min: 2D linear data interpolation with the size of (700x700) data elements.

Figure 10. Electrical bio-impedance tomography picture for skin exposed to US, 3 W/cm^2, for 4 min: 2D linear data interpolation with the size of (700x700) data elements.
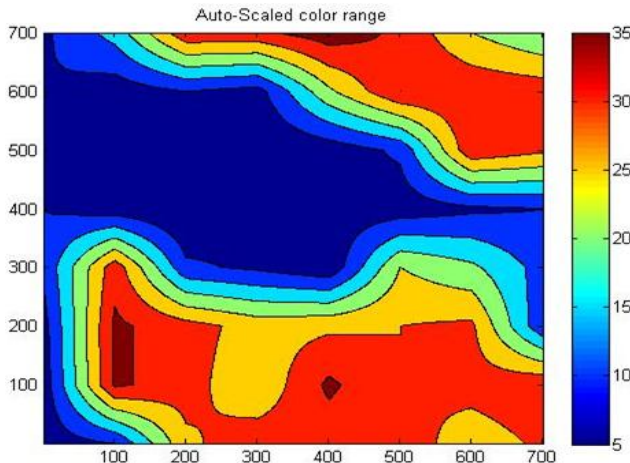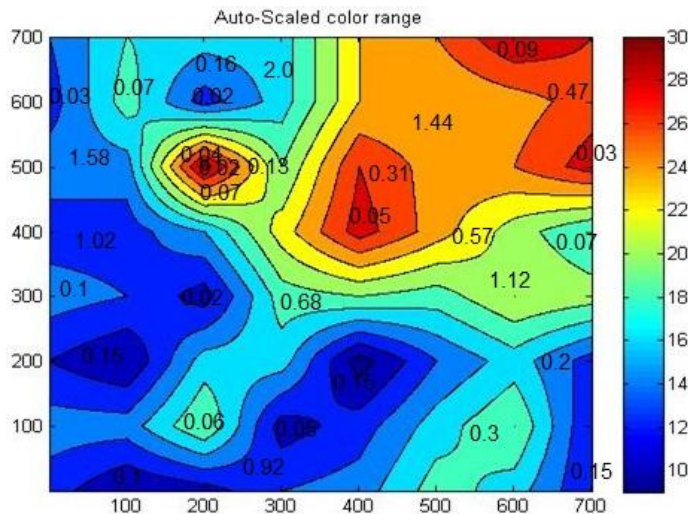

Figure 11. Electrical bio-impedance tomography picture for skin exposed to US, 3 W/cm^2, for 6 min. Area distribution in (inches)^2 obtained by area of polygon program is illustrated.

Table 1. Statistical analysis (averages and standard deviations) of the bio-impedance results.

Group	Control	US[*], 2min	US[*], 4min	US[*], 6min	US[**], 2min	US[**], 4min	US[**], 6min
Bioelectrical impedance	30.60±1.81	27.37±1.05	27.02±1.11	26.67±1.45	18.54±0.62	17.88±0.88	17.57±0.95

US[*]: Groups exposed to ultrasound 1 W/cm^2. US[**]: Groups exposed to ultrasound 3 W/cm^2.

example. Table 1 summarizes the statistical analysis of the impedance results.

DISCUSSION

There are a variety of medical problems for which it would be useful to know the time-varying distribution of electrical properties inside the body. High-conductivity materials allow the passage of both direct and alternating currents; high-permittivity materials allow the passage of only alternating currents. Both of these properties are of interest in medical applications, because different tissues have different conductivities and permittivities (Cancel et

al., 2004). The application of ultrasound (sonophoresis) has been shown to increase the low skin permeability for various drugs (Sarheed and Abdul Rasool, 2011). The mechanisms and applications of sonophoresis have been reviewed before (Polat et al., 2010). Cavitation, the growth and collapse of gas bubbles, is generally recognized to be the dominant mechanism of sonophoresis. Cavitation is thought to disorder the lipid bilayers in the outermost layer of the skin, the stratum corneum, creating mass transfer pathways and thus increasing the diffusion coefficient of solutes.

However, cavitation alone cannot account for the total mass transfer enhancement observed. Several mechanisms seem to contribute to this transport phenomenon, among them, structural changes caused by cavitation (Smith, 2007), thermal effects (Kalluri and Banga, 2011), mixing in the liquid phase (Levy et al., 1989) and acoustic streaming through hair follicles and sweat ducts (Tachibana and Tachibana, 1993). The electrical resistance of the skin is a good instantaneous indicator of the structural properties of the skin (Allenby et al., 1961). Due to significant hindrance of the ionic transport through the lipid bilayers, the electrical resistance of the skin is very high and, in most previous studies, it has been used to verify that the structural integrity of skin samples is within the normal range. So, the continuous monitoring of skin electrical resistance during ultrasound application can provide insight into the mechanisms governing the enhancement of mass transfer through this biological barrier. Tang et al. (2001) indicated that in the context of the porous pathway hypothesis, when the transport of a permeant occurs via pure diffusion, log P_{diff} versus log R should exhibit a linear behavior with a slope of -1. So, following up the skin electrical properties through different sonophoresis conditions will guide to a prediction of the optimum permeability conditions, and that was achieved through our usage of electrical impedance tomography. It was concluded from Figures 5 to 11 and Table 1 that EIT showed the difference in skin conductivity between control and sonophoretic groups. The complex impedance of the control group was significantly decreased due to sonophoretic exposure either for 1 or 3 W/cm^2. The P-values between control and groups exposed to 1 W/cm^2 for 2, 4, and 6 min were 0.0087, 0.0055, and 0.0053 respectively, while they were less than 0.0001 for 3 W/cm^2 at the same time intervals.

It was also noticed that there was no significant impedance decreases within the same power at the studied time intervals; the P-values at 1 W/cm^2 were 0.6223, 0.4074, 0.6795 as a comparison between 2, 4, 6 min respectively, and they were 0.2076, 0.0922, 0.6795 for 3 W/cm^2 at the same time intervals. These results may be because the used time intervals were narrow and more investigation in a wider range may be performed in the future. At each corresponding time of exposure, there was very high significant decrease in skin impedance at 3 W/cm^2 than 1 W/ cm^2 (all P-values were less than 0.0001) and that may be because higher powers cause higher

thermal effect, and due to the relatively higher coherence of thermal effect with cavitation in power of 3 W/cm^2 more decrease in skin impedance occurred. These results support the facts that EIT can be used to detect the impedance (or conductivity) change in the skin under sonophoresis exposure, which in turn can give the optimum conditions of exposure, as well as the idea that sonophoresis decreases skin resistance which in turn increases the permeability of solutes to the skin which has many bio-medical applications.

ACKNOWLEDGEMENT

REFERENCES

Allenby A, Schock C, Tees TF (1961). The effect of heat and organic solvents on the electrical impedance and permeability of excised human skin. Br. J. Dermatol., 81: 31–62.

Bagshaw P, Liston D , Bayford H, Tizzard A, Gibson P, Thomas A, Sparkes K, Dehghani H, Binnie D, Holder S (2003). Electrical impedance tomography of human brain function using reconstruction algorithms based on the finite element method. NeuroImage, 20: 752–764.

Bodenstein M, Matthias D, Markstaller K (2009). Principles of electrical impedance tomography and its clinical application. Crit. Care Med., 37: 713-724.

Cancel M, Tarbell M, Jebria A (2004). Fluorescein permeability and electrical resistance of human skin during low frequency ultrasound application. JPP. 56: 1109–1118.

Cheneyy M, Isaacsony D, Newell C (1993). Electrical Impedance Tomography. SIAM. Review, 41: 85–101.

Costaa LV, Limab R, Amato BP (2009). Electrical impedance tomography, Curr. Opin. Crit. Care, 15: 18–24.

Johnson ME, Blankschtein D, Langer R (1997). Evaluation of solute permeation through the stratum corneum: Lateral bilayer diffusion as the primary transport mechanism. J. Pharm. Sci., 86: 1162-1172.

Hadgraft J, Guy RH (1989). Transdermal drug delivery, New York, Marcel Dekker. Reference to a chapter in an edited book : Developmental issues and research initiatives.

Kalluri H, Banga AK (2011). Transdermal delivery of proteins, AAPS. Pharm. Sci. Tech., 12: 431-441.

Levy D, Kost J, Meshulam Y, Langer R (1989). Effect of ultrasound on transdermal drug delivery to rats and guineapigs. J. Clin. Invest., 83: 2074–2078.

Metherall P, Barber DC, Smallwood RH, Brown BH (1996). Three dimensional electrical impedance tomography. Nature, 380: 509–512.

Pahade A, Jadhav VM, Kadam VJ (2010). Sonophoresis: An Overview. Int. J. Pharm. Sci. Rev. Res., 3: 24-32.

Polat BE, Blankschtein D, Langer R (2010). Low-frequency sonophoresis: application to the transdermal delivery of macromolecules and hydrophilic drugs. Expert Opin. Drug Deliv., 7: 1415-1432.

Polat BE, Hart D, Langer R, Blankschtein D (2011). Ultrasound-mediated transdermal drug delivery: mechanisms, scope, and emerging trends. J. Control Release, 152: 330-348.

Prausnitz MR, Bose VG, Langer R, Weaver JC (1993). Electroporation of mammalian skin: A mechanism to enhance transdermal drug delivery. Proc. Nat. Acad. Sci., 90: 10504-10508.

Sarheed O, Abdul Rasool BK (2011). Development of an optimised application protocol for sonophoretic transdermal delivery of a model hydrophilic drug. Open Biomed. Eng. J., 5: 14-24.

Schaefer H, Redelmeier TE (1996). Skin barrier. Reference to a chapter in an edited book: principles of percutaneous absorption, K. Basel.

Smith NB (2007). Perspectives on transdermal ultrasound mediated drug delivery. Int. J. Nanomed., 2: 585-594.

Tachibana K, Tachibana S (1993). Use of ultrasound to enhance the local-anesthetic effect of topically applied aqueous lidocane. Anesthesiology, 78: 1091–1096.

Tang H, Mitragotri S, Blankschtein D, Langer R (2001). Theoretical Description of Transdermal Transport of Hydrophilic Permeants: Application to Low-Frequency Sonophoresis. J. Pharm. Sci., 90: 545-568.

Takasuga S, Yamamoto R, Mafune S, Sutoh C, Kominami K, Yoshida Y, Ito M, Kinoshita M (2011). *In-vitro* and *in-vivo* transdermal iontophoretic delivery of tramadol, a centrally acting analgesic. J. Pharm. Pharmacol., 63:1437-1445.